

Numerical Study on Monopole Production and Deconfinement Transition in Two-Condensate Charged Systems

Kai Kang ¹, Jie Li ², Guo Wang ², Jiangning Zhang ¹, Jiantao Che ^{1,2} , Tianyi Han ²  and Hai Huang ^{1,3,*}

¹ Department of Mathematics and Physics, North China Electric Power University, Beijing 102206, China
² School of Nuclear Science and Engineering, North China Electric Power University, Beijing 102206, China
³ Hebei Key Laboratory of Physics and Energy Technology, North China Electric Power University, Baoding 071000, China
* Correspondence: huanghai@ncepu.edu.cn

Abstract: The condensed matter Bose system may contain effective monopole quasiparticles in its excitation spectrum. In this paper, we first accomplish the mapping of the two-band Ginzburg–Landau theory to the extended CP¹ model, and then perform the Monte Carlo simulations on the 50 × 50 × 50 cubic lattice with periodic boundary conditions. With the numerical data of monopole density and magnetic susceptibility, we indicate that there exists a monopole–antimonopole deconfinement transition for the two-band superconducting system with the critical temperature above 70 K. We also suggest the possible detection of this new monopole plasma phase in high-*T_c* iron-based superconductors.

Keywords: extended CP¹ model; monopole production; deconfinement phase transition; Monte Carlo simulation



Citation: Kang, K.; Li, J.; Wang, G.; Zhang, J.; Che, J.; Han, T.; Huang, H. Numerical Study on Monopole Production and Deconfinement Transition in Two-Condensate Charged Systems. *Crystals* **2024**, *14*, 397. <https://doi.org/10.3390/cryst14050397>

Academic Editors: António José Arsénio Costa, Elkin Ferney Rodriguez Velandía and João Filipe Pereira Fernandes

Received: 26 March 2024
Revised: 22 April 2024
Accepted: 23 April 2024
Published: 25 April 2024



Copyright: © 2024 by the authors. Licensee MDPI, Basel, Switzerland. This article is an open access article distributed under the terms and conditions of the Creative Commons Attribution (CC BY) license (<https://creativecommons.org/licenses/by/4.0/>).

1. Introduction

Since Curie pointed out the conceivable existence of magnetic monopoles dated back to 1894 [1], continuous efforts have been devoted to looking for existent evidences and understanding physical properties of this elusive particle. In 1931, Dirac demonstrated the consistency of monopoles with quantum mechanics and that the presence of magnetic charge would explain the observed quantization of electric charge [2]. About forty years later, 't Hooft and Polyakov indicated independently that magnetic monopoles are actually predicted by all grand unified theories in elementary particle physics [3,4]. Meanwhile, the magnetic monopole can also be realized as an emergent particle due to the correlations present in strongly interacting condensed matter systems, such as a class of exotic magnets known collectively as spin ice [5]. With the improvement of experiment techniques, various predictions on magnetic monopoles have been readily proposed nowadays, and it is reasonable to expect that these progresses will greatly promote the detection of this mysterious particle.

With the discovery of two-band superconductivity at about 40 K in magnesium diboride [6], there has been a wide interest in condensed matter systems with several coexisting Bose condensates. For example, it has been argued that under certain conditions, even liquid metallic hydrogen might allow for superconductivity with both electronic and protonic Cooper pairs [7]. Theoretically, two charged condensates together with their electromagnetic interactions can be phenomenologically described by the two-band Ginzburg–Landau (GL) model. By presenting an explicit change in variables, it can be shown that there exists an exact mathematical equivalence between this GL theory and a version of the O(3) nonlinear σ -model [8]. This mapping is particularly interesting since it may give topological excitations in the form of stable, finite length knot solitons in the two-condensate charged system.

In the present paper, we will suggest that besides the knotted vortices mentioned above, another kind of topological defect, namely, monopole excitations, can also present in the two-condensate charged system. We show that the monopole or antimonopole excitation, which reflects the non-trivial winding of the phase difference between two complex order parameters, is allowed in the two-band GL theory. This quasiparticle, with the hedgehog (thus topological non-trivial) configuration, is similar to phonon excitation, which refers to the collective vibrations in crystals. At low temperatures, the monopole and antimonopole will form a tightly bound state due to the string tension between these quasiparticles. Then, with the increase in temperature, the two-condensate charged system will enter the so-called deconfinement phase, in which the thermal fluctuation will dominate the string tension, and the monopole and antimonopole pairs at the string endpoints will become nearly free particles. Therefore, we can observe a plasma phase of monopoles and antimonopoles in the sample above the deconfinement transition temperature. This deconfinement scenario is very similar to the two-dimensional Kosterlitz–Thouless phase transition of usual magnetic vortices.

Based on the two-band GL theory, we first transform the $O(3)$ nonlinear σ -model into the CP^1 form and then perform the Monte Carlo simulations with the so-called extended CP^1 model. Our numerical works on the monopole density and magnetic susceptibility indicate that there exists a monopole–antimonopole deconfinement transition for the two-band superconducting system with the critical temperature above about 70 K. We also discuss the possible detection of this monopole and antimonopole production in high- T_c iron-based superconductors.

The paper is organized as follows. In the next section, we introduce the two-band GL theory and its mathematical mapping to the extended CP^1 model. In Section 3, we give the lattice formulation of this CP^1 model and the procedure of Monte Carlo simulations. Then, in Section 4, we discuss the numerical results on the possible monopole–antimonopole deconfinement transition in the two-condensate charged system. Finally, Section 5 gives the conclusion of the paper.

2. Theoretical Scheme

We first write down the GL functional for two electromagnetically coupled Bose condensates as [8–11]

$$H = \sum_{\alpha=1,2} \left[\frac{\hbar^2}{2m_\alpha} \left| \left(\nabla - \frac{2ie}{\hbar c} \mathbf{A} \right) \Psi_\alpha \right|^2 + V(|\Psi_\alpha|) \right] + \frac{\mathbf{B}^2}{8\pi} \quad (1)$$

with

$$V(|\Psi_\alpha|) = -b_\alpha |\Psi_\alpha|^2 + \frac{c_\alpha}{2} |\Psi_\alpha|^4. \quad (2)$$

Here, Ψ_α and m_α separately represent the superconducting order parameter and effective mass for each band ($\alpha = 1, 2$). The magnetic field $\mathbf{B} = \nabla \times \mathbf{A}$ with \mathbf{A} as the vector potential, and b_α, c_α as temperature-dependent parameters.

We can introduce the variables ρ and χ_α as

$$\Psi_\alpha = \sqrt{2m_\alpha} \rho \chi_\alpha \quad (3)$$

where the complex $\chi_\alpha = |\chi_\alpha| e^{i\varphi_\alpha}$ are chosen so that $|\chi_1|^2 + |\chi_2|^2 = 1$. Then the modulus ρ takes the following expression

$$\rho^2 = \frac{1}{2} \left(\frac{|\Psi_1|^2}{m_1} + \frac{|\Psi_2|^2}{m_2} \right). \quad (4)$$

Now, we define a gauge invariant field $\mathbf{n} = \chi^\dagger \boldsymbol{\sigma} \chi$ with $\chi = (\chi_1, \chi_2)^T$ and $\boldsymbol{\sigma} = (\sigma_1, \sigma_2, \sigma_3)$ Pauli matrices, and write the supercurrent density in the following form:

$$\mathbf{j} = i[\chi_1 \nabla \chi_1^* - \chi_1^* \nabla \chi_1 + \chi_2 \nabla \chi_2^* - \chi_2^* \nabla \chi_2]. \quad (5)$$

With simple algebras, we can obtain two identities as follows:

$$\hbar^2 \rho^2 [(\nabla \chi_1)^2 + (\nabla \chi_2)^2] - \frac{1}{4} \hbar^2 \rho^2 \mathbf{j}^2 = \frac{1}{4} \hbar^2 \rho^2 (\nabla \mathbf{n})^2 \quad (6)$$

and

$$(\nabla \times \mathbf{j})_i = \frac{1}{2} \epsilon_{ijk} \mathbf{n} \cdot \partial_j \mathbf{n} \times \partial_k \mathbf{n} \quad (7)$$

with $i, j, k = 1, 2, 3$. Note that the Einstein summation is assumed here.

Following Ref. [8], we can then identify the \mathbf{n} -field part of the Hamiltonian in Equation (1) as a version of the O(3) nonlinear σ model

$$H_0 = \frac{\hbar^2 \rho^2}{4} (\nabla \mathbf{n})^2 + \frac{\hbar^2 c^2}{512 \pi e^2} (\epsilon_{ijk} \mathbf{n} \cdot \partial_j \mathbf{n} \times \partial_k \mathbf{n})^2. \quad (8)$$

In order to conveniently perform the numerical simulations, we will transform Equation (8) into the CP¹ form. In the CP¹ representation, we introduce a complex two-component spinor $z = (z_1, z_2)^T$, which is defined by the following formula:

$$\mathbf{n} = z^\dagger \boldsymbol{\sigma} z \quad (9)$$

with $z^\dagger z = 1$. With the introduction of a new gauge field $\mathbf{a} = -iz^\dagger \nabla z$, the O(3) nonlinear σ -model can be rewritten in the CP¹ form as

$$\frac{\hbar^2 \rho^2}{4} (\nabla \mathbf{n})^2 = \hbar^2 \rho^2 [(\nabla + i\mathbf{a})z^\dagger][(\nabla - i\mathbf{a})z]. \quad (10)$$

In Equation (10), there is a local gauge invariance under the transformation

$$z(\mathbf{r}) \rightarrow e^{i\gamma(\mathbf{r})} z(\mathbf{r}) \quad (11)$$

and

$$\mathbf{a} \rightarrow \mathbf{a} + \nabla \gamma(\mathbf{r}) \quad (12)$$

with arbitrary function $\gamma(\mathbf{r})$.

Based on the explicit vortex solution of the CP¹ model, the corresponding vector potential on a spatial plane reads

$$\mathbf{a} = \nabla \phi \sin^2\left(\frac{u}{2}\right) \quad (13)$$

with the cylindrical coordinate (r, ϕ) . Here, the function $u(r)$ satisfies the condition $u(0) = \pi$. Then, the vortex flux going through a circle C of radius r is

$$\Phi(r) = \oint_C \mathbf{a} \cdot d\mathbf{l} = 2\pi \sin^2\left(\frac{u}{2}\right). \quad (14)$$

At $r \rightarrow 0$, we have the magnetic flux as 2π . Therefore, we can identify the vortex as a configuration in which the spatial plane is pierced by a singular flux tube. The Dirac string is just the world line of flux tube in the three-dimensional Euclidean space, and the magnetic monopole and antimonopole are the source and sink of these flux tubes in the three-dimensional space. The monopole or antimonopole solution takes the hedgehog configuration $\mathbf{n}(\mathbf{r}) = z^\dagger \boldsymbol{\sigma} z = \pm \mathbf{r}/r$ as shown in Figure 1. Note that both vortex and monopole solutions represent the non-trivial winding of the phase difference between two complex order parameters in the two-condensate charged system.

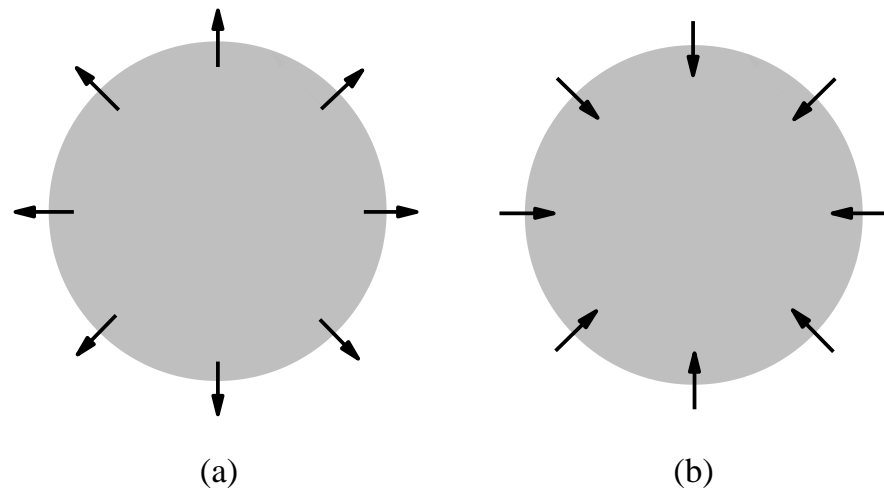


Figure 1. The hedgehog configurations of a monopole (a) and an antimonopole (b) in the O(3) nonlinear σ -model or the CP¹ model.

With the definition of an artificial magnetic field $\mathbf{b} = \nabla \times \mathbf{a}$, we can show from Equation (9)

$$\mathbf{b}_i = \frac{1}{4} \epsilon_{ijk} \mathbf{n} \cdot \partial_j \mathbf{n} \times \partial_k \mathbf{n}. \quad (15)$$

Then, the Hamiltonian in Equation (8) can be written as

$$H_0 = \hbar^2 \rho^2 [(\nabla + \mathbf{ia})z^\dagger][(\nabla - \mathbf{ia})z] + \frac{\hbar^2 c^2}{32\pi e^2} \mathbf{b}^2, \quad (16)$$

which we call the extended CP¹ model with the extra magnetic energy term in the above expression. Physically, the vector potential \mathbf{a} and the artificial magnetic field \mathbf{b} in the CP¹ model reflect the space variation of the phase difference between two order parameters in the GL theory or the phase coherence between two different types of Cooper pairs in the electronic structure. The extra magnetic energy term emerges from the gradient part of the GL free energy functional in Equation (1), and it reveals the additional energy contribution of the non-trivial phase difference variations in the three-dimensional space.

3. Lattice Formulation And Monte Carlo Simulations

Now, we try to put this system on a three-dimensional cubic lattice with periodic boundary conditions. For simplicity, we set the lattice constant $a = 1$ in this section. A complex two-component spinor z_r of the unit norm is attached to each site r . Let \mathbf{i} denote the lattice vector $\hat{\mathbf{r}}_i$, and the connection defined as

$$V_r^i = z_r^\dagger z_{r+i} \quad (17)$$

will approach $1 + \mathbf{ia}_i$ in the naive continuum limit [12]. Therefore, the covariant derivative $(\nabla - \mathbf{ia})$ can be latticized as

$$(\nabla - \mathbf{ia})_i z(\mathbf{r}) \rightarrow z_{r+i} - V_r^i z_r \quad (18)$$

and

$$[(\nabla + \mathbf{ia})_i z^\dagger(\mathbf{r})][(\nabla - \mathbf{ia})_i z(\mathbf{r})] \rightarrow 1 - |z_r^\dagger z_{r+i}|^2. \quad (19)$$

More precisely, the gauge field \mathbf{a}_r^i associated with a link \mathbf{i} at site r can be defined as

$$e^{i\mathbf{a}_r^i} = V_r^i / |V_r^i| \quad (20)$$

with $-\pi < a_r^i < \pi$. The curl of the gauge field shows its sum around an oriented plaquette, which is specified by a site r and two different directions i and j . Note the order of directions also identifies its orientation here. For this plaquette, the curl can be decomposed into the following form:

$$(\nabla \times \mathbf{a})_r^{ij} = \mathbf{a}_r^i + \mathbf{a}_{r+i}^j - \mathbf{a}_{r+j}^i - \mathbf{a}_r^j = f_r^{ij} + 2\pi n_r^{ij}, \quad (21)$$

where the field strength f_r^{ij} satisfies $-\pi < f_r^{ij} < \pi$ and the integer n_r^{ij} represents the vortex number of the plaquette (r, ij) . Then, the magnetic field on the lattice can be defined as

$$\mathbf{b}_r^i = \frac{1}{2} \epsilon_{ijk} (\nabla \times \mathbf{a})_r^k. \quad (22)$$

Combining Equations (19) and (22) and dropping a constant term, we can obtain the lattice action from the Hamiltonian in Equation (16)

$$H_{\text{latt}} = - \sum_{r,i} \left[\hbar^2 \rho^2 |z_r^\dagger z_{r+i}|^2 - \frac{\hbar^2 c^2}{32\pi e^2} \mathbf{b}_r^2 \right]. \quad (23)$$

And the partition function is given by

$$Z = \int D\mathbf{z} e^{-H_{\text{latt}}/k_B T} \quad (24)$$

with k_B the Boltzmann constant.

Monopoles are defined as sources of the magnetic field, and the monopole number m_r in a cube attached to r is given through the relation

$$(\nabla \cdot \mathbf{b})_r = \sum_i [\mathbf{b}_{r+i}^i - \mathbf{b}_r^i] = 2\pi m_r. \quad (25)$$

Due to the periodic boundary conditions, there must be an equal number of monopoles and antimonopoles, i.e.,

$$\sum_r m_r = 0. \quad (26)$$

As a result, we can deduce that a monopole must be connected to an antimonopole by an unbroken string of vortices as illustrated in Figure 2. This string represents the world line of a vortex in the three-dimensional Euclidean space.

Based on the lattice action in Equation (23), we then perform the Monte Carlo simulations on the $50 \times 50 \times 50$ periodic lattice space. At each site r , we first generate a random 2×2 SU(2) matrix and take the first column to be the spinor z_r [13–15]. With the conventional Metropolis algorithm [16,17], the updating procedure is as follows. Choose a configuration at random as a candidate for the new configuration. If it lowers the energy, accept it; otherwise, accept it with probability $\exp(-\Delta E/k_B T)$, where ΔE is the increase in energy between these two configurations. This updating procedure can kick a system into a higher energy state and simulate thermal fluctuations. In practice, one updates the lattice configuration one link at a time. Thus, the computation of energy differences will only involve the plaquettes containing this updated link. In our numerical computations, the first 10^6 sweeps are discarded to ensure thermalization and 10^7 iterations are used to calculate our physical quantities in a run.

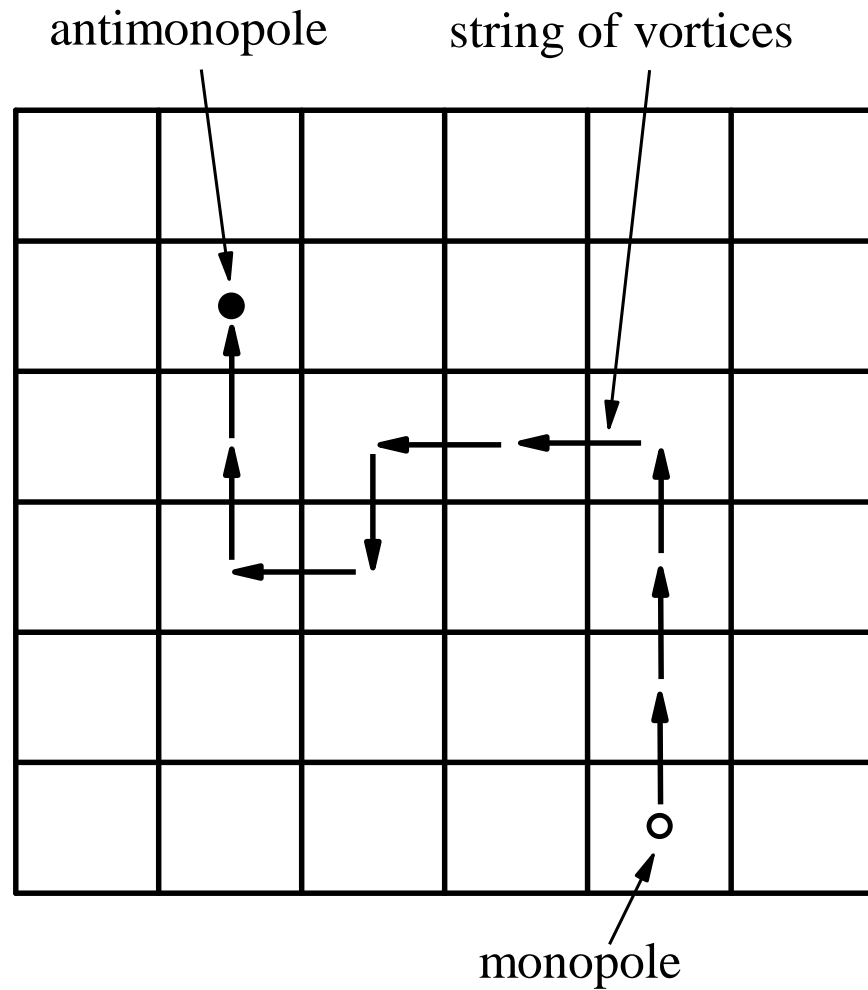


Figure 2. A schematic of vortex string run from a monopole to an antimonopole on the lattice space.

4. Monopole–Antimonopole Deconfinement Transition

Now, we can study the monopole and antimonopole pair productions in the two-condensate charged system based on the Monte Carlo procedure mentioned above. To simulate the realistic two-band superconductors, we take the zero-temperature coherence length $\xi_0 \sim 100$ nm as the lattice spacing. In this circumstance, we can approximate $\hbar^2 \rho^2 = \hbar^2 \rho_0^2 (1 - T/T_c)$ with $\hbar^2 \rho_0^2 \sim 0.01$ eV · nm^{−1} and T_c , the superconducting critical temperature in the GL theory [18,19].

First, we define the absolute magnitude of the magnetization per site as

$$M = \left\langle \sum_r |m_r| \right\rangle, \quad (27)$$

which gives the probability of finding a monopole or antimonopole in the elementary cube. Based on the lattice action in Equation (23), we perform the numerical computations at $T_c = 100$ K and plot the results in Figure 3. From Figure 3, we can see that M shows a rapid increase to about 0.26 around $T_d \approx 86$ K. It clearly indicates that there exists a monopole–antimonopole deconfinement phase transition at T_d . We also note that we have never found a monopole configuration with $|m_r| > 1$ in our numerical simulations.

We also calculate the monopole susceptibility

$$\chi = \frac{dM}{dT} \quad (28)$$

and plot the results at $T_c = 100$ K in Figure 4. From Figure 4, we can see the monopole susceptibility shows a sharp peak at T_d , which is consistent with the monopole density data.

At this point, we would like to point out that no magnetic monopole exists in the continuum limit of the three-dimensional volume for two-condensate charged systems. As we know, the monopole solution corresponds to a hedgehog configuration in the $O(3)$ nonlinear σ -model or the CP^1 model. Detailed calculation shows that the solution of the monopole and antimonopole pair presents the ultraviolet divergence in the action, but this short wavelength fluctuation can be regulated by a natural cutoff, i.e., the lattice spacing in the condensed matter systems.

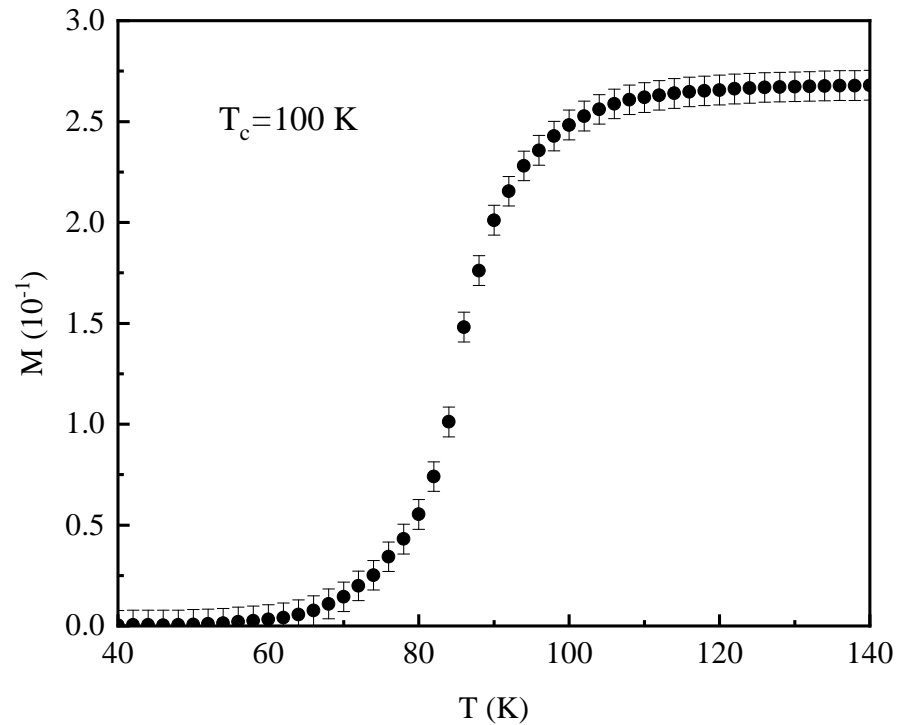


Figure 3. The temperature dependence of monopole density for the two-condensate charged system with $T_c = 100$ K.

Finally, we also compute the monopole–antimonopole deconfinement transition temperature T_d as a function of the superconducting critical temperature T_c . The results are plotted in Figure 5. From Figure 5, we can see that due to the magnetic energy term in Equation (23), the possible monopole and antimonopole production at $T \in (T_d, T_c)$ will only exist above $T_c \approx 70$ K, and T_d increases to about 115 K as T_c reaches 130 K. Since the discovery of the F-doped superconductor $LaFeAsO_{1-x}F_x$ with $T_c \sim 26$ K in 2008 [20], other Fe-based superconducting systems have also generated great interest in the scientific community. The parent compounds of these superconductors are usually semi-metallic and the contribution of all five $3d$ electrons to the Fermi surface manifests the multi-band electronic structure in the materials. Up to now, the highest known critical temperature of about 58 K has been achieved in the two-band iron pnictide $SmFeAsO_{1-x}F_x$ [21]. Thus, it is very promising that we will experimentally observe the monopole plasma phase from the multi-band Fe-based superconductors in the near future.

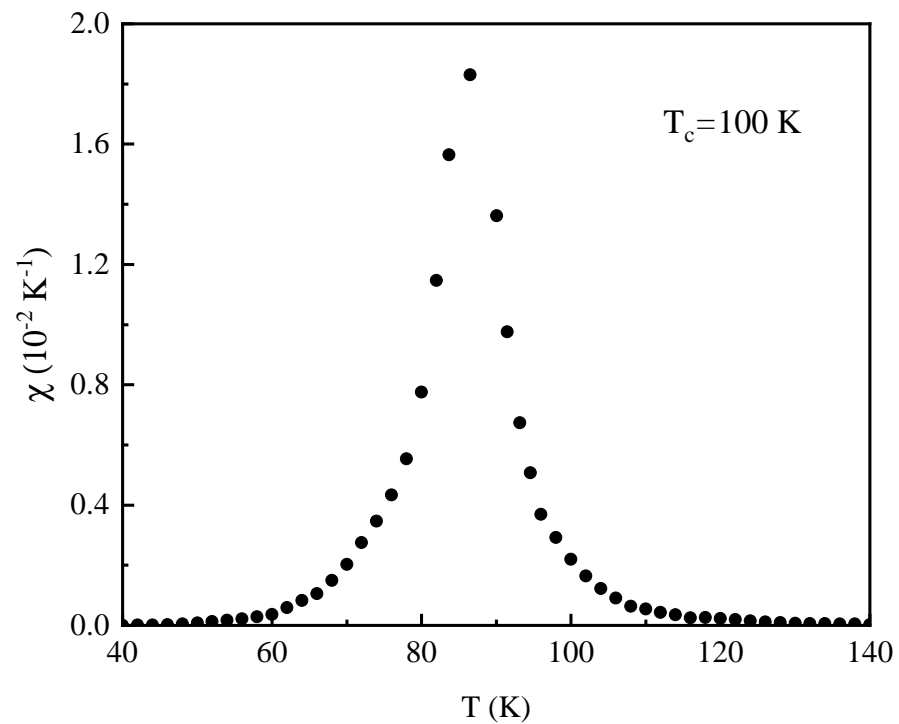


Figure 4. The temperature dependence of magnetic susceptibility for the two-condensate charged system with $T_c = 100 \text{ K}$.

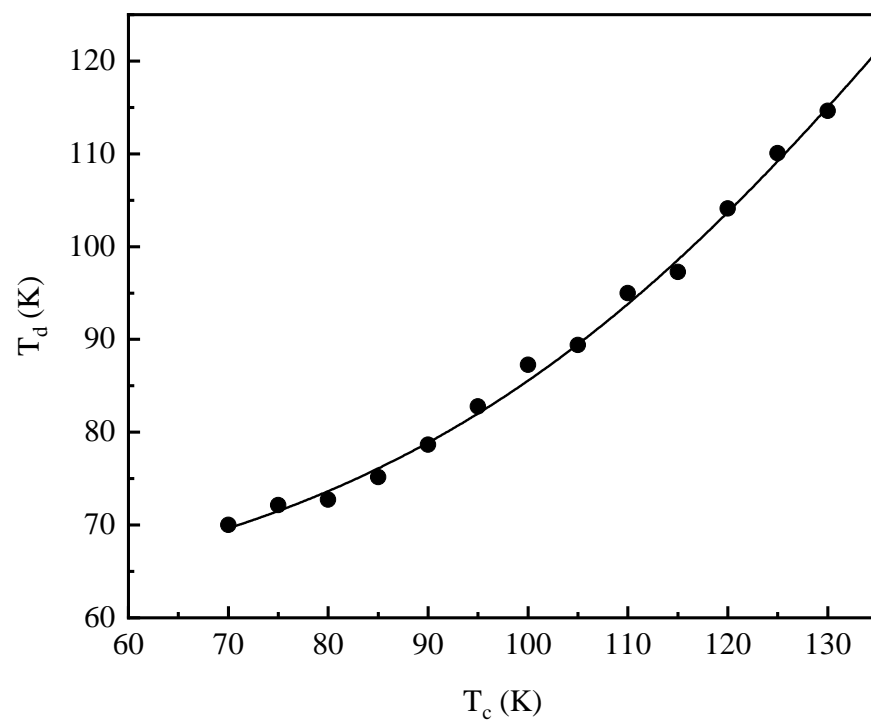


Figure 5. The monopole deconfinement transition temperature T_d as a function of T_c .

5. Conclusions

In summary, based on the extended CP^1 model, we have studied the topological monopole excitations in the three-dimensional two-condensate charged system. Our numerical data on the monopole density and magnetic susceptibility indicate that there exists a monopole–antimonopole deconfinement transition for the two-band superconducting system

with a critical temperature of above about 70 K. We also suggest the possible experimental detection of this monopole plasma phase in high- T_c iron-based superconductors.

Author Contributions: Conceptualization, K.K., J.L., G.W., J.Z., J.C., T.H. and H.H.; methodology, K.K., J.L., G.W., J.Z., J.C., T.H. and H.H.; software, K.K., J.L. and G.W.; validation, K.K., J.L., G.W., J.Z., J.C., T.H. and H.H.; formal analysis, K.K., J.L., G.W. and J.Z.; investigation, K.K., J.L., G.W., J.Z., J.C., T.H. and H.H.; resources, H.H.; data curation, K.K., J.L. and H.H.; writing—original draft preparation, K.K.; writing—review and editing, K.K., J.L., G.W., J.Z., J.C., T.H. and H.H.; visualization, K.K.; supervision, J.C., T.H. and H.H.; project administration, H.H. All authors have read and agreed to the published version of the manuscript.

Funding: This research received no external funding.

Data Availability Statement: Data are contained within the article.

Conflicts of Interest: The authors declare no conflicts of interest.

References

1. Curie, P. On the possible existence of magnetic conductivity and free magnetism. *J. Phys. Theor. Appl.* **1894**, *3*, 415. [[CrossRef](#)]
2. Dirac, P.A.M. Quantised singularities in the electromagnetic field. *Proc. R Soc. London A* **1931**, *133*, 60.
3. 't Hooft, G. Magnetic monopoles in unified gauge theories. *Nucl. Phys. B* **1974**, *79*, 276. [[CrossRef](#)]
4. Polyakov, A.M. Particle spectrum in the quantum field theory. *JETP Lett.* **1974**, *20*, 194.
5. Castelnovo, C.; Moessner, R.; Sondhi, S.L. Magnetic monopoles in spin ice. *Nature* **2008**, *451*, 42. [[CrossRef](#)] [[PubMed](#)]
6. Nagamatsu, J.; Nakagawa, N.; Muranaka, T.; Zenitani, Y.; Akimitsu, J. Superconductivity at 39 K in magnesium diboride. *Nature* **2001**, *410*, 63. [[CrossRef](#)] [[PubMed](#)]
7. Mouloupoulos, K.; Ashcroft, N.W. Coulomb interactions and generalized pairing in condensed matter. *Phys. Rev. B* **1999**, *59*, 12309. [[CrossRef](#)]
8. Babaev, E.; Faddeev, L.D.; Niemi, A.J. Hidden symmetry and knot solitons in a charged two-condensate Bose system. *Phys. Rev. B* **2002**, *65*, 100512. [[CrossRef](#)]
9. Askerzade, I.N.; Gencer, A.; Güçlü, N. On the Ginzburg-Landau analysis of the upper critical field H_{c2} in MgB₂. *Supercond. Sci. Technol.* **2002**, *15*, L13. [[CrossRef](#)]
10. Doh, H.; Sigrist, M.; Cho, B.K.; Lee, S. Phenomenological theory of superconductivity and magnetism in Ho_{1-x}Dy_xNi₂B₂C. *Phys. Rev. Lett.* **1999**, *83*, 5350. [[CrossRef](#)]
11. Zhitomirsky, M.E.; Dao, V.-H.; Ginzburg-Landau theory of vortices in a multigap superconductor. *Phys. Rev. B* **2004**, *69*, 054508. [[CrossRef](#)]
12. Vecchia, P.D.; Nicodemi, F.; Pettorino, R.; Veneziano, G. Large N , chiral approach to pseudoscalar masses, mixings and decays. *Nucl. Phys. B* **1981**, *181*, 318. [[CrossRef](#)]
13. Berg, B.; Stehr, J. SU(2) lattice gauge theory and Monte Carlo calculations. *Z. Phys. C Part. Fields* **1981**, *9*, 333. [[CrossRef](#)]
14. Martinelli, G.; Parisi, G.; Petronzio, R. Monte Carlo simulations for the two-dimensional O(3) non-linear sigma model. *Phys. Lett. B* **1981**, *100*, 485. [[CrossRef](#)]
15. Azcoiti, V.; Nakamura, A. Monte Carlo simulation of SU(2) lattice gauge theory with internal quark loops. *Phys. Rev. D* **1983**, *27*, 2559(R). [[CrossRef](#)]
16. Metropolis, N.; Ulam, S. The Monte Carlo method. *J. Am. Stat. Assoc.* **1949**, *44*, 335. [[CrossRef](#)] [[PubMed](#)]
17. Creutz, M. Lattice gauge theories and Monte Carlo algorithms. *Nucl. Phys. B* **1989**, *10*, 1. [[CrossRef](#)]
18. Tinkham, M. *Introduction to Superconductivity*; McGraw-Hill Inc: New York, NY, USA, 1996.
19. de Gennes, P. G. *Superconductivity of Metals and Alloys*; Westview Press: New York, NY, USA, 1966.
20. Kamihara, Y.; Watanabe, T.; Hirano, M.; Hosono, H. Iron-based layered superconductor La[O_{1-x}F_x]FeAs ($x = 0.05$ – 0.12) with $T_c = 26$ K. *J. Am. Chem. Soc.* **2008**, *130*, 3296. [[CrossRef](#)] [[PubMed](#)]
21. Fujioka, M.; Denholme, S.J.; Ozaki, T.; Okazaki, H.; Deguchi, K.; Demura, S.; Hara, H.; Watanabe, T.; Takeya, H.; Yamaguchi, T.; et al. Phase diagram and superconductivity at 58.1 K in α -FeAs-free SmFeAsO_{1-x}F_x. *Supercond. Sci. Tech.* **2013**, *26*, 085023. [[CrossRef](#)]

Disclaimer/Publisher's Note: The statements, opinions and data contained in all publications are solely those of the individual author(s) and contributor(s) and not of MDPI and/or the editor(s). MDPI and/or the editor(s) disclaim responsibility for any injury to people or property resulting from any ideas, methods, instructions or products referred to in the content.